Production of porous ceramic material using different sources of alumina and calcia

Ivone Regina de Oliveira [1], Vitoria Marques Cesar Leite [1],
Milene Paula Vargas Porto Lima [1], Rafael Salomão [2]

[1] Institute for Research and Development, University of Vale do Paraiba, São José dos Campos, SP
e-mail: ivonero@univap.br
[2] Materials Engieering Department, São Carlos School of Engineering, University of São Paulo, São Carlos, SP
e-mail: rsalomao@sc.usp.br

ABSTRACT

Numerous papers and publications report the use of microporous calcium hexaluminate ($CaO.6Al_2O_3$; CA_6) as a key raw material for high temperature insulating materials. This material has unique properties with respect to chemical purity and mineral composition. Another important property of CA_6 is its structure, which consists of platelet-shaped crystals that interlock. The free distance between the crystals defines the microporous structure. The low density in combination with the micropores hampers heat transfer by radiation at temperatures exceeding 1000 ^{o}C and results in a low thermal conductivity. Given the advantages presented by this material, it is necessary to understand the formation mechanism of CA_6 grains in order to better develop the potential applications of this material. CA_6 can be fabricated using organic binders to consolidate the Al_2O_3-$CaCO_3$ powder mixture and to provide green strength so that a green body can be formed and retains the desired shape before heating. However, these organic binders must be completely thermally decomposed so that they do not remain in the sintered body as carbon or ash. Moreover, the use of organic binders releases large volumes of gases such as carbon dioxide from the green body during heating. Therefore, an eco-friendly ceramic fabrication process has been developed that employs an inorganic binder (hydraulic alumina). The aim of the present work was to study the synthesis of porous calcium-hexaluminate ceramics using calcined alumina or hydraulic alumina combined with different sources of calcia ($CaCO_3$ and $Ca(OH)_2$) at different temperatures. The materials produced were characterized by X-ray diffraction, scanning electron microscopy, apparent porosity and mercury intrusion porosimetry. The materials produced by hydraulic alumina presented higher porosity and larger pores compared to those produced from calcined alumina.

Keywords: Calcium hexaluminate, synthesis, inorganic binder, properties.

1. INTRODUCTION

Ceramic fiber-based materials are widely employed as thermal insulators for high temperature applications (above 1200°C) due to their low thermal conductivity and thermal shock resistance. Recently, due to their potential for causing lung diseases and allergies, efforts have been made to replace these materials by non-fiber containing alternatives [1-4]. The microporous monolithic ceramics are the most important candidates [5]. Differently from the fiber-based boards, in porous monolithics, the ceramics matrixes comprise sintered particles surrounding micro-to-macro porous. Due to this, this class of materials presents low thermal conductivity and reduces the generation of hazardous dust during installation and use. Recent studies report porous calcium hexaluminate structures as suitable candidates for this application [1-5].

Calcium hexaluminate ($CaAl_{12}O_{19}$, $CaO.6Al_2O_3$, or simply CA_6), also known as hibonite, is an alumina-rich intermediate compound of the CaO-Al_2O_3 system, with high thermal stability and refractoriness (melting point of 1830°C) [1,4-7]. It is formed according with the general expression:

$$6Al_2O_3 + CaO \rightarrow CaAl_{12}O_{19} \qquad (1)$$
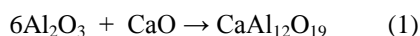
Considering its use for thermal insulation, CA_6 has three important and simultaneous advantages over other systems: 1) it presents intrinsic resistance for densification, therefore, preventing densification of the structure during use at high temperatures [8]; 2) it allows the generation of structures with large volume of microporous and homogeneous microstructure [4-6]; and 3) due to its plate-like crystalline habit provides high fracture energy and thermal shock resistance [3-5].

The difficulties in sintering and densification of CA_6 were described in studies focused in producing dense optical devices and were attributed to multiple aspects. In sintering pre-formed CA_6, the densification difficulties are associated with the plate-like shape of its particles and with the large average crystal size and their high stability. Furthermore, because CA_6 is a solid solution with broad range of composition, the absence of second phases at the grain boundaries easies grain growth instead of densification as main sintering mechanism. For *in situ* generation by solid-state reaction (between precursors such as CaO and Al_2O_3), other aspects also impede sintering. CA_6 formation is a double-diffusion mechanism, where Ca^{2+}, Al^{3+}, and O^{2-} ions are mutually exchange amongst the particles. Because there are significant differences between the diffusion rates of Ca^{2+} in Al_2O_3 and Al^{3+} in CaO, the overall kinetics of the reaction is slow and several intermediate compounds can be formed and decomposed before reaching the desired composition. In addition, due to the density mismatch of reactants (ρAl_2O_3 = 4 g.cm^{-3}) with (ρCaO = 3.5 g.cm^{-3}) and CA_6 (ρ = 3.2 g.cm^{-3}), its formation is followed by a volumetric expansion that can keep particles apart, preventing densification.
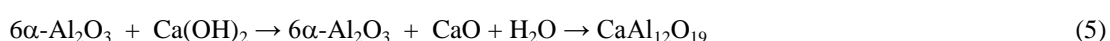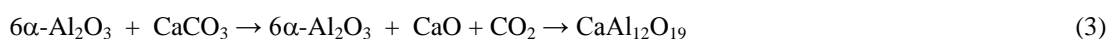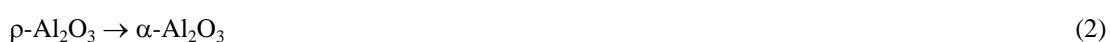
Regarding the thermal shock behavior, insulating materials experience severe stresses during use caused by sudden temperature variations. Usually, these stresses are high enough to generate and propagate catastrophic cracks all over the structure. In CA_6 systems, on the other hand, crack propagation is impeded by the microporous and tortuous structure. Due to this, these materials present high thermal shock resistance despite their low density [3,4] allowing the production of very complex and large-sized components [4]. Even under severe conditions, for example exposure to harsh thermal shock conditions or alkali attack, service life has by far exceeded initial expectations [3,7]. This interesting combination of high refractoriness and thermomechanical performance allows CA_6 to be used in many industrial applications such as refractories for steel and glass making, non-ferrous foundry and petrochemical unities [3,7,9].

The pores formation in CA_6 structures can be carried out by two main routes. The first is the compacting and sintering of pre-formed CA_6 generating the so-called light-weight aggregates. Some variations that include the introduction of organic porogenic (such as starch) or foamed suspensions (using surfactants) are also possible [8]. Because of the high energy consumption of the pre-formed material, alternative routes have been developed, such as the combination of Al_2O_3 and $CaCO_3$ precursors [6,8]. In these cases, the pore generation occurs during the decomposition reactions and can be partially preserved during sintering. Despite the high porosity levels achieved, the use of carbonated precursors inevitably produces CO_2 as by-product.

Searching for a more environmentally-friend system, this study aimed to produce porous CA_6 structures combining alternative Al_2O_3-CaO sources: calcined Al_2O_3 (α-Al_2O_3) and hydraulic Al_2O_3 (ρ-Al_2O_3) and CaO (decomposed $CaCO_3$) and $Ca(OH)_2$, respectively. After sintering at different temperatures, physical and morphological characterizations were carried out. The results attained were related to the properties and characteristics of the precursor raw materials.

2. MATERIALS AND METHODS

Calcined alumina (CA, α-Al_2O_3, A1000SG, Almatis, USA), hydraulic alumina (HA, ρ-Al_2O_3, Alphabond 300, Almatis, USA), calcium carbonate ($CaCO_3$, Vetec, Brazil), and calcium hydroxide ($Ca(OH)_2$, Synth, Brazil) were used as reactants. The morphology of particles was analysed by scanning electron microscopy (EVO MA10; Zeiss) as showing in Figure 1. Others characteristics of the materials are presented in Table 1. Raw materials were mixed accordingly to their chemical composition (Table 2) to produce calcium hexaluminate following the general expressions:
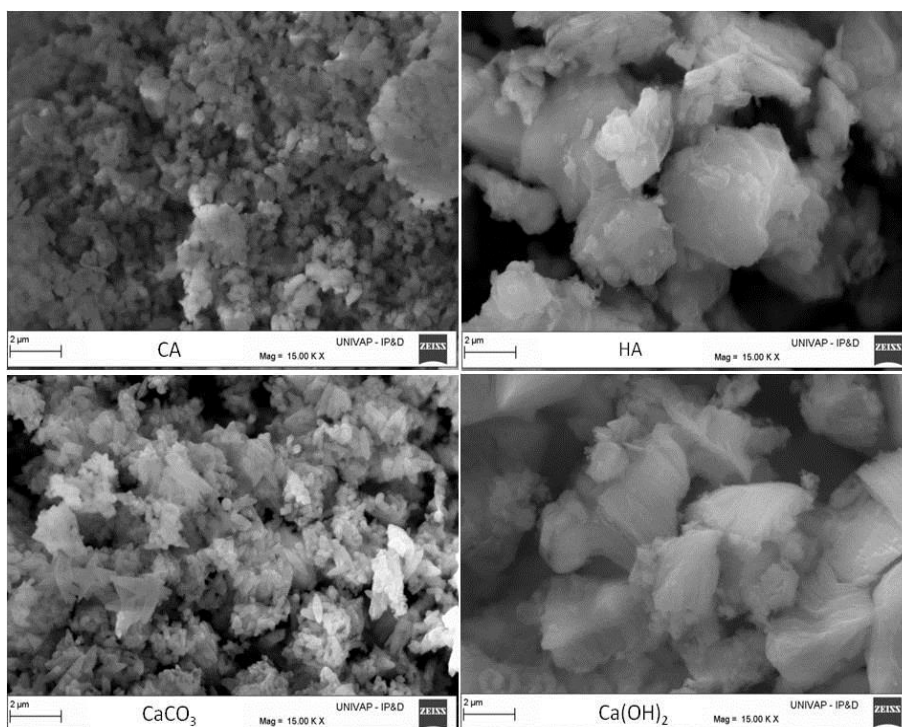
$$\rho\text{-}Al_2O_3 \rightarrow \alpha\text{-}Al_2O_3 \tag{2}$$

$$6\alpha\text{-}Al_2O_3 + CaCO_3 \rightarrow 6\alpha\text{-}Al_2O_3 + CaO + CO_2 \rightarrow CaAl_{12}O_{19} \tag{3}$$

$$6\alpha\text{-}Al_2O_3 + CaO \rightarrow CaAl_{12}O_{19} \tag{4}$$

$$6\alpha\text{-}Al_2O_3 + Ca(OH)_2 \rightarrow 6\alpha\text{-}Al_2O_3 + CaO + H_2O \rightarrow CaAl_{12}O_{19} \tag{5}$$

Figure 1: Scanning electron microscopy for as-received particles calcined alumina (CA), hydraulic alumina (HA), $CaCO_3$ and $Ca(OH)_2$.

Table 1: Characteristics of the raw materials

	Calcined alumina (CA, α-Al_2O_3)	Hydratable alumina (HA, ρ-Al_2O_3)	Calcium carbonate ($CaCO_3$)	Calcium hydroxide ($Ca(OH)_2$)
Solid density (g.cm^{-3})	3.95	2.72	2.83	2.21
Specific surface area (m^2.g^{-1})	7.0	95	-	-
Particle size (D_{50}/D_{90}, μm)	0.5 / 1.2	10 / 23	2.2 / 3.8	6.5 / 13
Composition (wt.%)	Al_2O_3: 99.8; Na_2O: 0.08; Fe_2O_3: 0.02; SiO_2: 0.03; CaO: 0.02; MgO: 0.07	Al_2O_3: 99.4; Na_2O: 0.5; Fe_2O_3: 0.02; SiO_2: 0.03; CaO: 0.02; MgO: 0.07	$CaCO_3$: 99.0; Sr: 0.1; Na: 0.1;SO_4: 0.01; K: 0.01; Mg: 0.02; Fe: 0.003; NH_4: 0.003; Cl: 0.001; Ba: 0.005; F: 0.0015	$Ca(OH)_2$: 95.0; CO_3: 3.0; Cl: 0.03; SO_4: 0.1; Fe: 0.05

The different mixtures (CA-$CaCO_3$, CA-$Ca(OH)_2$, HA-$CaCO_3$, and HA-$Ca(OH)_2$) were initially homogenized in a ball-mill for 5 hours (6 mm corundum spheres were used as milling agent in a 5:1 ratio; no fluid or additives were added to this system) and then uniaxially pressed as cylinders of 20 mm diameter by 6 mm height. Sintering was performed at 1550, 1600, and 1650ºC for 2 h (heating and cooling rate of 5ºC.min^{-1}) using an oven (Lindberg Blue, U.S.A.).

Table 2: Evaluated conditions for the production of calcium hexaluminate

ALUMINA SOURCE	CALCIUM SOURCE	PROPORTIONS (wt%)	SINTERING TEMPERATURE (^{o}C)
CA	$CaCO_3$	85.9:14.1	1550, 1600
	$Ca(OH)_2$	89.0:11.0	1550, 1600
HA	$CaCO_3$	88.0:12.0	1550, 1600,1650
	$Ca(OH)_2$	90.5:9.5	1550, 1600,1650

The apparent porosity level of the sintered samples was measured by immersion tests using Archimedes' principle, using water as immersion fluid. This principle states that an immersed body is buoyed up by a force equal to the weight of the displaced fluid. The buoyant force is measured by the difference (expressed in grams) between the weight of the body in air and when submerged in water [10]. The samples were initially weighed dried (W_d, g). After 1 hour of immersion in water under vacuum atmosphere, samples were weighed inside the immersion liquid (W_i, g). Next, the excess liquid was removed with a humid blanket and the samples were weight again (W_h, g). The apparent porosity (AP, %) was calculated considering the mass of liquid retained in its open pores:

$$AP = 100\% \times [(W_h - W_d)/(W_h - W_i)] \tag{6}$$

Pore size distribution of samples was determined by mercury intrusion porosimetry (Autopore IV 9500, Micromeritics). In this technique, a non-wetting liquid (mercury) is forced to penetrate the pores of the structure. The volume of mercury intruded into the pores can be measured directly as a function of the applied pressure (P) using the Washburn equation:

$$D = -4\gamma P^{-1}\cos(\phi) \tag{7}$$

where, D is the pore diameter (μm), P is the applied pressure (Pa), γ is the surface tension of mercury (mN.m^{-1}), and ϕ is the contact angle (130º) between the mercury and the sample. Varying the pressure level applied, the pore size distribution can be determined.

X-ray diffraction (XRD-6000, Shimadzu; CuKα radiation = 1.54439 Å) was performed in crushed samples ($D_{Part} < 100$ μm) to indentify the phases formed and the microstructure at the external surface of the sintered samples was investigated by means of scanning electron microscopy (SEM, EVO MA10, Zeiss, previously covered by thin gold coating).

3. RESULTS AND DISCUSSION

In situ reactions in the CaO-Al_2O_3 system have been extensively studied due to its importance in the production of calcium aluminate cement (CAC). These studies revealed that, depending on the reacting condition (particle size, degree of mixing, average distance amongst particles, mineraliser additives, time-temperature, and cooling rate), several intermediate compounds (such as $C_{12}A_7$) with different composition can be formed before the CA_6 stoichiometry is reached. In the present work, all sintered samples presented a XRD pattern similar to the pre-formed commercial electrofused CA_6 grade, formed by a single and highly crystalline phase (Figure 2). These results indicate that the conditions employed favored the full conversion of the Al and Ca sources into CA_6.
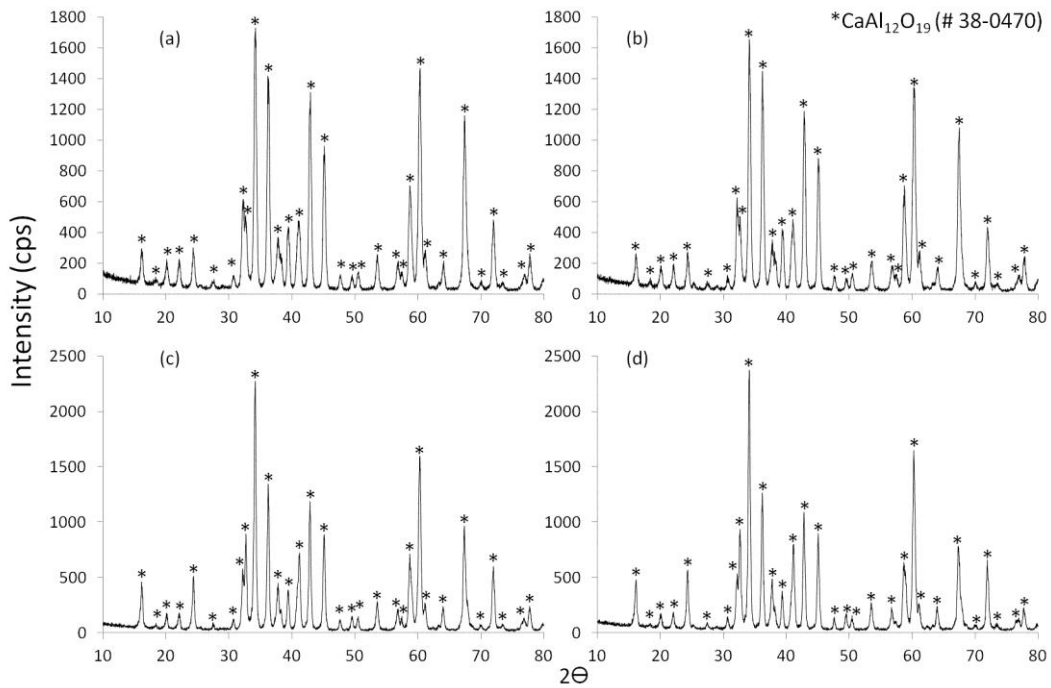
Figure 2: DRX patter for sample prepared by mixing (a) CA-CaCO$_3$ (85.9:14.1), (b) CA-Ca(OH)$_2$ (89.0:11.0) sintered at 1600 ^{o}C, and (c) HA-CaCO$_3$ (88.0:12.0), (d) HA-Ca(OH)$_2$ (90.5:9.5) sintered at 1650 ^{o}C (* = JCPDS file 38-0470)

Different apparent porosity levels (Figure 3) and average pore size (AVP, Figure 4) were achieved after thermal treatment depending on samples' composition and sintering temperatures.

The greatest porosity levels and AVP were achieved for the HA-containing samples sintered at 1550ºC. For the same Al$_2$O$_3$ source (CA or HA), samples with previously formed CaO (calcined CaCO$_3$) presented porosity levels slightly higher. Despite the distinct composition, because this variation in porosity is smaller than 10 percent points, it can be attributed mainly to effects related to packing efficiency at the green state. Greater differences were observed between the different Al$_2$O$_3$ sources: HA containing samples presented porosity levels and AVP almost twice as high as the equivalent CA containing ones.
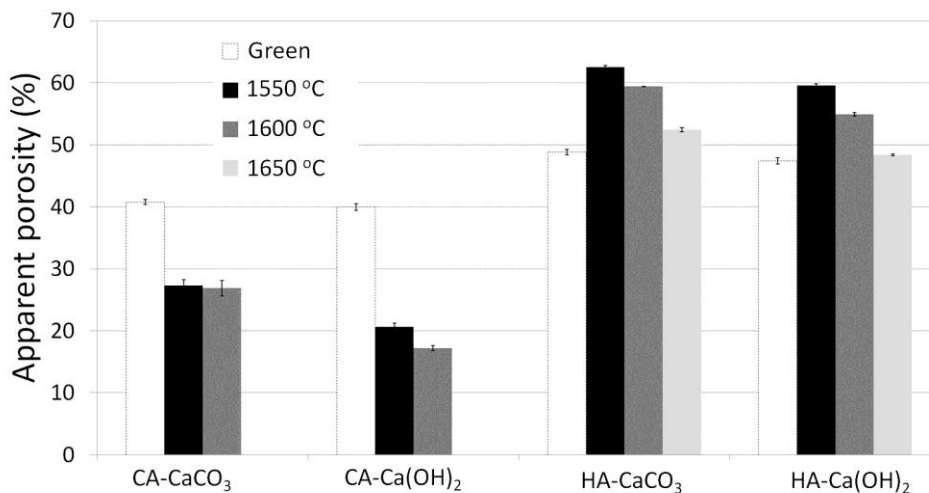

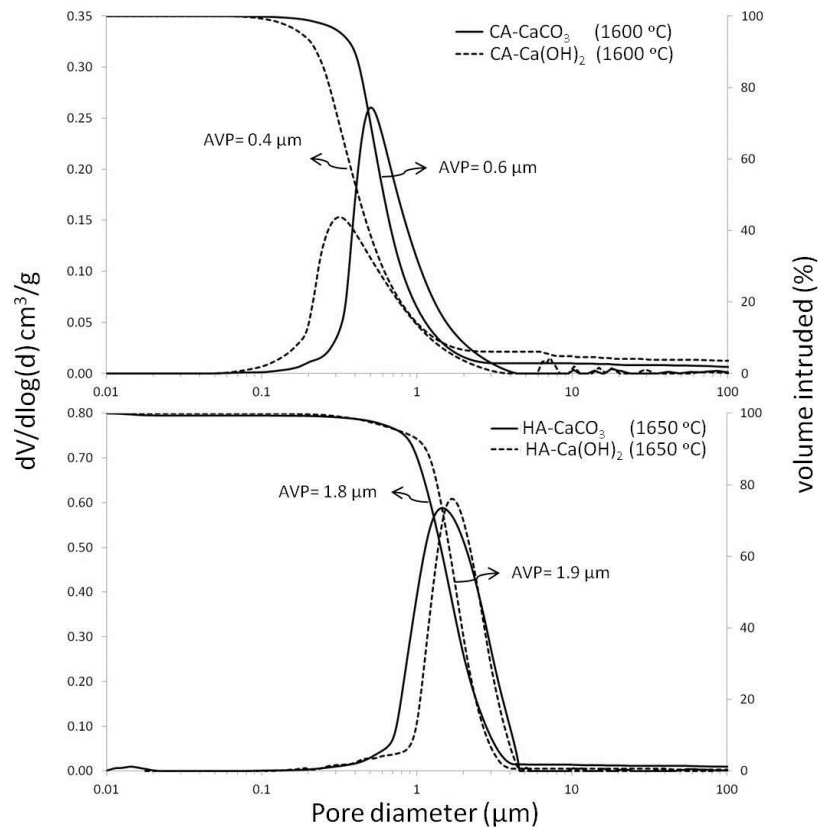**Figure 3:** Apparent porosity for samples green and sintered at different temperatures.

Figure 4: Pore size distribution for samples CA-CaCO$_3$ (85.9:14.1), CA-Ca(OH)$_2$ (89.0:11.0) sintered at 1600 ^{o}C, and HA-CaCO$_3$ (88.0:12.0), (d) HA-Ca(OH)$_2$ (90.5:9.5) sintered at 1650 ^{o}C.

Since alumina sources are the major component of the compositions, it is reasonable to consider that these results can be attributed to the physicochemical differences between them. Firstly, because hydratable alumina presents larger average particle size and specific surface area compared to the calcined alumina (Table 1), its packing efficiency is significantly lower which generates high porosity at the green samples (Figure 3). Secondly, whereas calcined alumina is a highly stable compound (formed entirely by the α-Al$_2$O$_3$ phase), hydratable alumina is comprised by ρ-Al$_2$O$_3$ phase that typically contains 10-15 wt% of chemically bonded water. At temperatures above 250°C, ρ-Al$_2$O$_3$ turns into boehmite and, at higher temperatures, into other transition phases of alumina. During this process, the significant density increase (from 2.8 g.cm^{-3} up to 3.5 g.cm^{-3}) behaves as porogenic mechanism, also reported elsewhere [11]. The combination of these effects causes the enhancement of the average space amongst the HA and CaO particles, comparing to the CA and CaO ones.

Because CA$_6$ formation is a solid-state diffusion-based reaction, during the first stages of sintering, particles densification is hindered. Besides this, since this reaction occurs mainly at contact points amongst the particles, the average size ratio between the alumina and calcia sources plays an important role. When coarse alumina particles (such as HA) are surrounded by thin calcia ones, at temperatures around 1400°C, calcium alumina (CA) is preferentially formed at the contact points, generating a small portion of liquid phase. As the sintering process carries on, this liquid dissolves more alumina from the neighboring particles precipitating other alumina rich compounds: CA$_2$ initially and CA$_6$ latter. Probably due to the large amount of liquid phase formed on the contact region, these crystals tend to be thicker and more regular. For a combination of thin particles (CA plus CaCO$_3$), on the other hand, due to the larger number of contact points, the reaction occurs more likely as a solid-state diffusion, with low generation of liquid phases. Due to this, the atomic interdifusion occurs mainly at few high energy crystallographic planes, generating more asymmetrical crystals that growth until impinge upon each other. This mechanism is schematically shown on Figure 5.

The development of CA$_6$ grains with different morphology can be explained in terms of distinct CA$_6$ reaction mechanisms, resulting from differences in the reactivity of the powders [12]. In this work, samples CA-CaCO$_3$ presented a platelet structure, whereas for the HA-CaCO$_3$ ones, a more equiaxial morphology was observed, as showing at Figure 6.
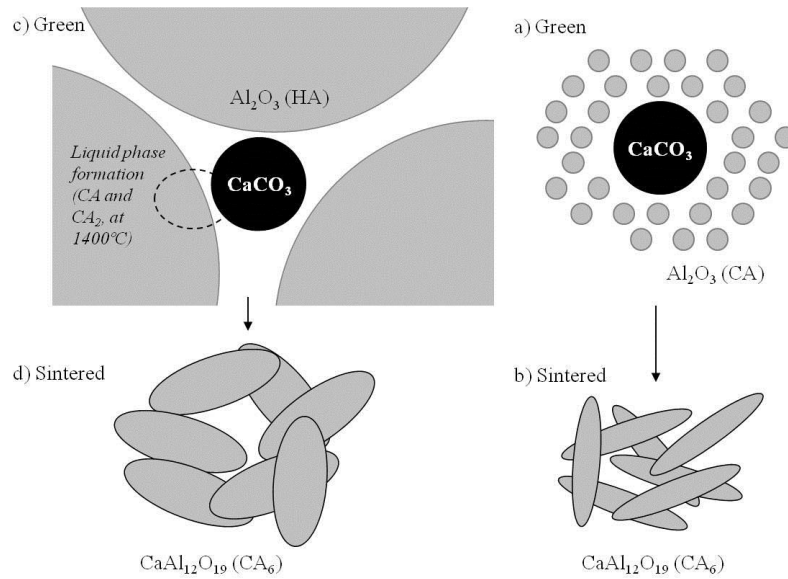
Figure 5: Schematic illustration of the reaction between the alumina and calcia sources for samples: (a, b) CA-CaCO$_3$ and (c, d) HA-CaCO$_3$ green and sintered at different temperatures.
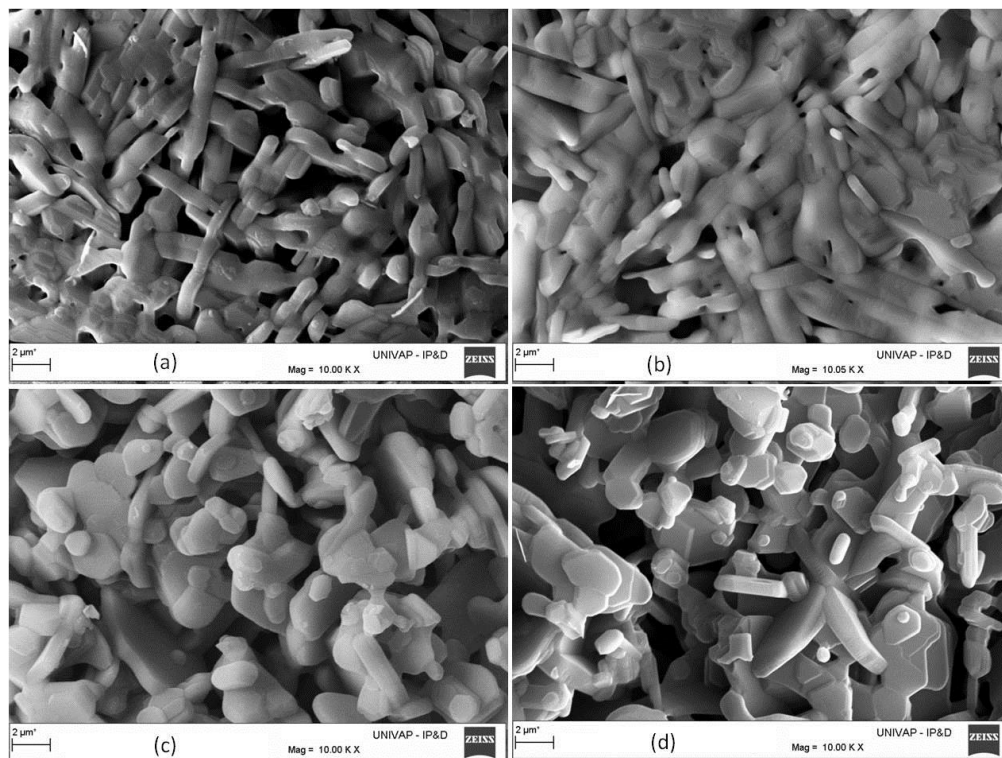

Figure 6: Scanning electron microscopy for samples (a) CA-CaCO$_3$ (85.9:14.1), (b) CA-Ca(OH)$_2$ (89.0:11.0) sintered at 1600 ^{o}C, and (c) HA-CaCO$_3$ (88.0:12.0), (d) HA-Ca(OH)$_2$ (90.5:9.5) sintered at 1650 ^{o}C.

4. CONCLUSIONS

Mixtures of different sources of Al$_2$O$_3$ and CaO (CA-CaCO$_3$, CA-Ca(OH)$_2$, HA-CaCO$_3$, HA-Ca(OH)$_2$) were used for synthesize porous CA$_6$ structures with a wide range of porosity and pore size distribution. High levels of porosity (~ 60 %) and small average pore size (1 µm) were obtained even for samples sintered at the highest sintering temperatures (1600 and 1650°C). The microstructures attained were strongly affected by the precursor raw materials. The grain morphology depends of calcium and alumina distributions in green spec-

imens as well as their characteristics (average particle size and surface area). Reactions between CA and calcium sources result in platelet grains, while HA result in grains with curved boundaries and higher porosity. Finally, it was demonstrated that $Ca(OH)_2$ is a suitable CO_2-free alternative for replacing $CaCO_3$ (or CaO produced from $CaCO_3$) in CA_6 synthesis.

5. ACKNOWLEDGMENTS

6. BIBLIOGRAPHY

[1] GARSEL, D. V., GNAUCK,V., KRIECHBAUM, G. W., *et al*., "New insulating raw material for high temperature applications", In: Proceedings of 41 International Colloquium on Refractories, pp. 122-128, Aachen, 1998.

[2] GARSEL, D. V., BUHR, A., GNAUCK, V., "Long term high temperature stability of microporous calcium hexaluminate based insulating materials", In: Proceedings of 42 International Colloquium on Refractories, pp. 181-186, Berlin, 1999.

[3] LORENZ, R. K., BUHR, A., RACHER, R. P., "Industrial application experiences with microporous calcium hexaluminate insulating material SLA-92", In: Proceedings of 48 International Colloquium on Refractories, pp. 66-70, 2005.

[4] OVERHOFF, A., BUHR, A., "New microporous materials for use in modern firing plants, cfi/Ber", *DKG*, v. 82, n. 8, pp. E1- E5, 2005.

[5] WIT, T., LORENZ, W., PORZGEN, D., *et al*., "Innovative ceramic fiber free steel ladle preheaters at Corus Steelworks IJ muiden", In: Proceedings of 44 International Colloquium on Refractories, pp. 108-112, Aachen, 2001.

[6] DOMINGUEZ, C., CHEVALIER, J., TORRECILLAS, R., *et al*., "Microstructure development in calcium hexaluminate", *Journal of the European Ceramic Society*, v. 21, pp. 381-387, 2001.

[7] SCHNABEL, M., BUHR, A., CHEL, G. B., *et al*., "Advantages of calcium hexaluminate in a corrosive environment", *Refractories WorldForum*, v. 3, n. 4, pp. 87-94, 2011.

[8] NAGAOKA, T., TSUGOSHI, T., HOTTA, Y., *et al*., "Forming and sintering of porous calcium-hexaluminate ceramics with hydraulic alumina", *Journal Material Science*, v. 41, pp. 7401-7405, 2006.

[9] AMTHAUER, K., BUHR, A., SCHNABEL, M., *et al*., "New european sinter aggregate with 96% Al_2O_3", In: Proceedings of 54th International Colloquium on Refractories – Refractories for Industrials, pp. 95-98, Aachen, Germany, 2011.

[10] FRIDLAND, M., ROSADO, R., "Mineral trioxide aggregate (MTA) solubility and porosity with different water-to-powder ratios", *Journal of Endodontics*, v. 29, pp. 814-817, 2003.

[11] SOUZA, A. D. V., SOUSA, L. L., FERNANDES, L., *et al*., "Al_2O_3–$Al(OH)_3$-Based castable porous structures", *Journal of the European Ceramic Society*, v. 35, n. 6, pp. 1943-1954, 2014.

[12] AN, L., CHAN, H. M., SONI, K. K., "Control of calcium hexaluminate grain morphology in *in-situ* toughened ceramic composites", *Journal of Materials Science*, v. 31, n.12, pp. 3223-3229, 1996.